Broken Bars And/Or End Rings Detection In Three-Phase Induction Motors By The Extended Park's Vector Approach

A. Aboubou (1) M. Sahraoui(1) S. E. Zouzou(1)
H. Razik(2) A. Rezzoug(2)

(1)M.S.E. Laboratory, University Med KHIDER
BP145, 07000 Biskra, Algeria
e-mail: aboubou_nacer@hotmail.com
(2) GREEN-UHP UMR 7037, University Henri Poincaré
BP 239, F-54506 Vandœuvre les Nancy, Cedex, France
e-mail: Hubert.Razik@green.uhp-nancy.fr

Abstract— **In this paper, we present a method dedicated to the detection of broken bars and end-rings defects in a three-phase induction motor. This method is based on the spectral analysis of the stator current Park's vector modulus. The theoretical principles of this method are described. Simulation and experimental results demonstrate the effectiveness of this method for the detection of the squirrel cage faults.**

I. Introduction

The asynchronous squirrel cage induction motor is a key component of the majority of the industrial plants, because of its great robustness and its low cost. It is indeed, omnipresent in the industrial sectors like aeronautics, the nuclear power, chemistry. In spite of these qualities. stresses of various natures (thermal, electric, mechanical or environment) can affect the life span of this one, by involving the occurrence of stator and/or rotor faults [11], [12].

These faults cause considerable economic losses. Thus, it is imperative to implement monitoring systems in order to avoid the unforeseen stops.

Malfunctions of a three-phase induction motor can be due to:

- **Rotor faults:**
  - Broken bars,
  - Broken end rings,
  - Air gap eccentricity,
  - Bearing faults.
- **Stator faults:**
  - Inter-turn short-circuits between,
  - Inter-phases short-circuits,
  - Cut of a phase.

The great development in the equipment and the software of the signal processing returned possible the diagnosis of the defects in the electrical machines. The principle of these new techniques of diagnosis is based on the localization of the spectral signatures characterizing the faults in the spectrum of signals, which are taken from the machine. Each defect appears either by the creation of harmonics at frequencies related to the nature of the defect, or by the modification of the amplitudes of the harmonics already presents in the spectrum [6], [8], [13].

According to the literature, the principal signals used to obtain information on the health of the machine are as follows:

- Stator current [5], [6], [13],
- Electromagnetic torque [9], [14],
- Mechanical vibration [10],
- Instantaneous power [4], [7].

Research concerning the use of the Park's vector approach [1], [2], demonstrated the effectiveness of this technique for the diagnosis of the abnormalities.

The development of the mathematical equations is made in a reference frame related to the rotor. It represents the contribution of the authors of this article.

II. The Extended Park's Vector Approach

The Park's vector components (i_{ds} and i_{qs}), in a reference frame related to the rotor ($\theta = \omega_r t$), can be expressed as a function of the stator current phases by:

$$\begin{cases} i_{ds}(t) = \sqrt{\frac{2}{3}}[i_a(t)\cos\theta + i_b(t)\cos(\theta - \frac{2\pi}{3}) \\ \qquad + i_c(t)\cos(\theta - \frac{4\pi}{3})] \\ i_{qs}(t) = \sqrt{\frac{2}{3}}[i_a(t)\sin\theta + i_b(t)\sin(\theta - \frac{2\pi}{3}) \\ \qquad + i_c(t)\sin(\theta - \frac{4\pi}{3})] \end{cases} \quad (1)$$

Under ideal conditions (without faults), the stator currents i_a, i_b and i_c are purely sinusoidal signals:

$$
\begin{cases}
i_a(t) = i_m \cos(\omega_s t - \alpha) \\
i_b(t) = i_m \cos(\omega_s t - \alpha - \frac{2\pi}{3}) \\
i_c(t) = i_m \cos(\omega_s t - \alpha - \frac{4\pi}{3})
\end{cases}
\quad (2)
$$

Under abnormal conditions (presence of a rotor defect for example), harmonics in the torque are generated, accompanied by oscillations in the speed and a modulation of the stator current [3][2]. Spectral components at $(1\pm 2ks)f_s$, characterizing this type of defect, appear in the line currents that still represent a multi-frequency three-phases symmetrical system. If only the first sideband components around the supply component at pulsation ω_s are considered, they can be expressed as:

$$
\begin{cases}
i_a(t) = i_f \cos(\omega_s t - \alpha) + i_l \cos[(1-2s)\omega_s t - \beta_l] \\
\qquad + i_r \cos[(1+2s)\omega_s t - \beta_r] \\
i_b(t) = i_f \cos(\omega_s t - \alpha - \frac{2\pi}{3}) + i_l \cos[(1-2s)\omega_s t - \beta_l - \frac{2\pi}{3}] \\
\qquad + i_r \cos[(1+2s)\omega_s t - \beta_r - \frac{2\pi}{3}] \\
i_c(t) = i_f \cos(\omega_s t - \alpha - \frac{4\pi}{3}) + i_l \cos[(1-2s)\omega_s t - \beta_l - \frac{4\pi}{3}] \\
\qquad + i_r \cos[(1+2s)\omega_s t - \beta_r - \frac{4\pi}{3}]
\end{cases}
\quad (3)
$$

With:

i_f: Maximum value of the fundamental supply phase current.
i_l: Maximum value of the lower sideband component $(1-2s)f_s$.
i_r: Maximum value of the higher sideband component $(1+2s)f_s$.
α: The phase angle of the fundamental supply phase current.
β_l: The phase angle of the current lower sideband component $(1-2s)f_s$
β_r: The phase of the current higher sideband component $(1+2s)f_s$

By replacing currents i_a, i_b and i_c by its expressions in the relation (1), we obtain:

$$
\begin{cases}
i_{ds}(t) = \sqrt{\frac{3}{2}} \left\{ \underbrace{i_f \cos[(s.\omega_s t - \alpha] + i_l \cos(-s.\omega_s t - \beta_l)}_{A1} + \underbrace{i_r \cos(3s.\omega_s t - \beta_r)}_{A2} \right\} \\
i_{qs}(t) = \sqrt{\frac{3}{2}} \left\{ \underbrace{i_f \sin[s.\omega_s t - \alpha] + i_l \sin(-s.\omega_s t - \beta_l)}_{A1} + \underbrace{i_r \sin(3s.\omega_s t - \beta_r)}_{A2} \right\}
\end{cases}
\quad (4)
$$

Under these conditions, it is clear that the two components i_{ds} and i_{qs} are made up of two parts:

- 1[rst] **part A1:** It contains two components at the frequency of sf_S
- 2[2nd] **part A2:** It contains a component at the frequency of $3sf_S$

Generally, the fracture of one or more bars generates in the spectrum of currents i_{ds} and i_{qs} a chain of harmonics at frequencies ksf_s with k=1, 3, 5... (Figure 1).

The square of the Park's vector modulus is given by:

$$
\begin{aligned}
\left| i_{ds} + j\, i_{qs} \right|^2 &= \frac{3}{2}(i_f^2 + i_l^2 + i_r^2) + 3 i_f i_l \cos(2s.\omega_s t - \alpha + \beta_l) \\
&+ 3 i_f i_r \cos(2s.\omega_s t - \alpha + \beta_r) \\
&+ 3 i_r i_l \cos(4s.\omega_s t + \beta_l - \beta_r)
\end{aligned}
\quad (5)
$$

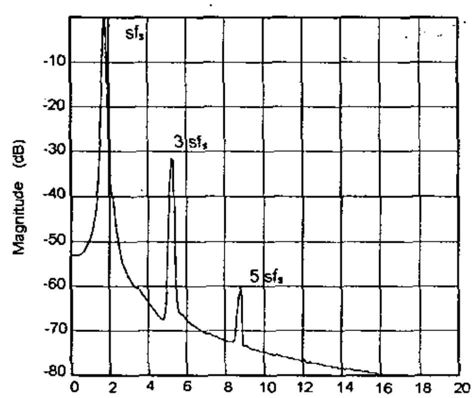

Fig.1 The spectrum of i_{ds} component for a motor with two broken bars (s=3,5%)

It is noticed that the spectrum of the current Park's vector modulus is the sum of "dc" level generated mainly by the fundamental component and a "ac" level that contains two terms at frequencies of $2sf_s$ and $4sf_s$. The "ac" level of the current Park's vector modulus is clear from any component at the fundamental supply frequency; it calls a characteristic component and it provides an extra piece of diagnostic information about the health of the motor.

Figure 2, shows that the occurrence of bars faults is characterized by the appearance of the components $2sf_s$ and $4sf_s$. These characteristic components can easily be distinguished and their amplitudes indicate the severity of the fault.

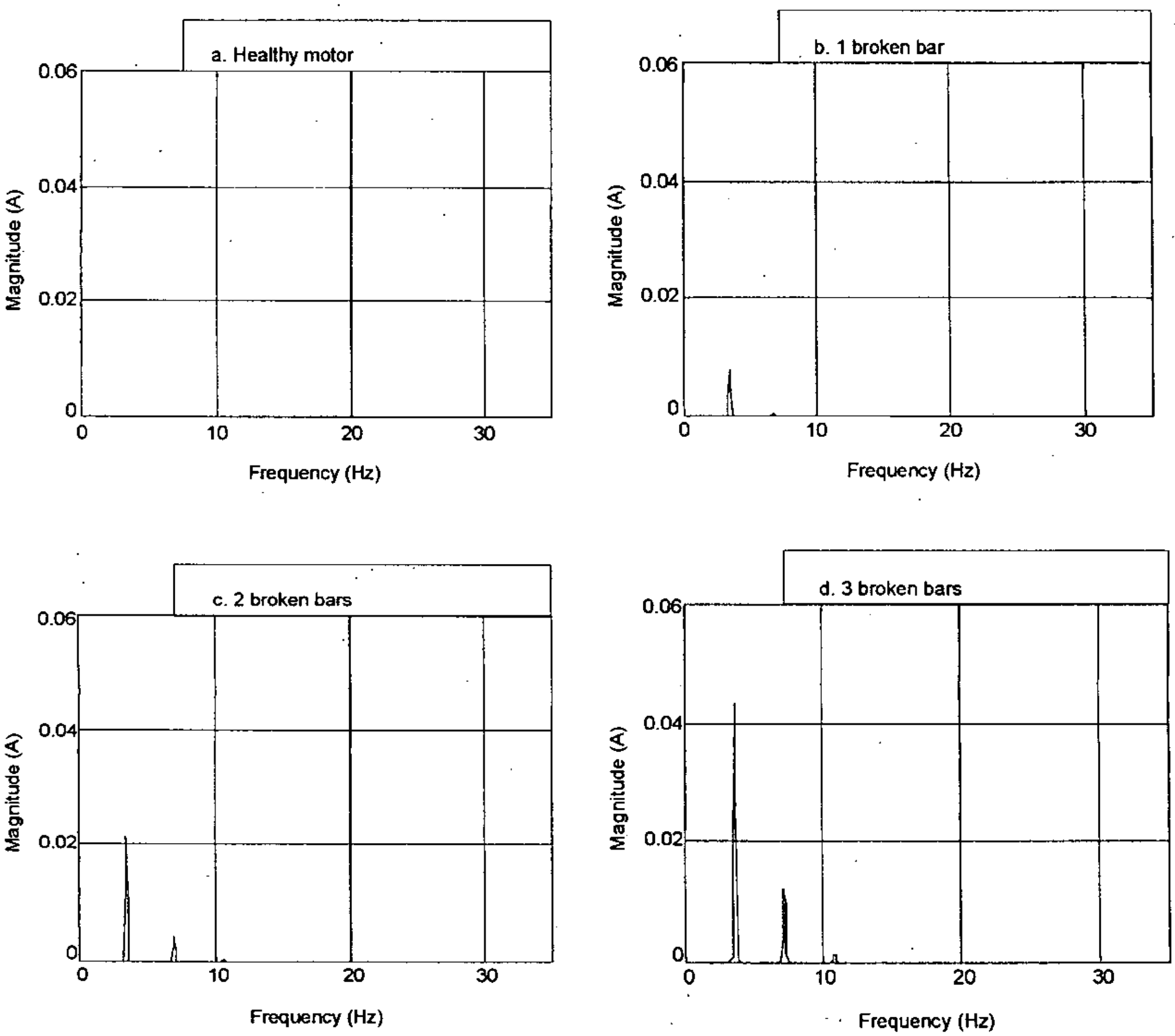

Fig.2 Simulation spectrum of the ac level of current Park's vector modulus for a motor with rated load

Figure 3 represents the spectrum of the ac level of the current Park's vector modulus; during the fracture of one then tows end rings. According to amplitudes of the harmonics $2ksf_s$, one can note that this kind of faults is more severe than that due to the broken bars.

To see moreover meadows severity of the default; we tried to see the variation of the amplitude of the harmonic $2sf_s$ according to the increase in the number of broken bars.

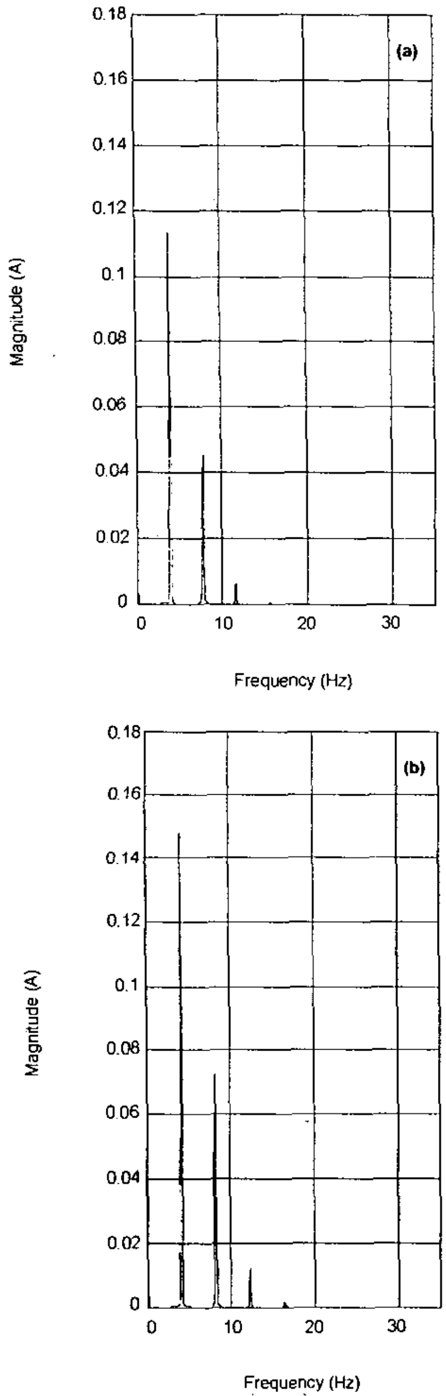

Fig.3 Simulation spectrum of the ac level of current Park's vector modulus corresponding to:
a. One broken end ring. b. Two broken end rings.

Figure 4 shows that there is an increase in the magnitude of the $2sf_s$ component with the extension of the faults, making this component a good indicator of the conditions of the motor.

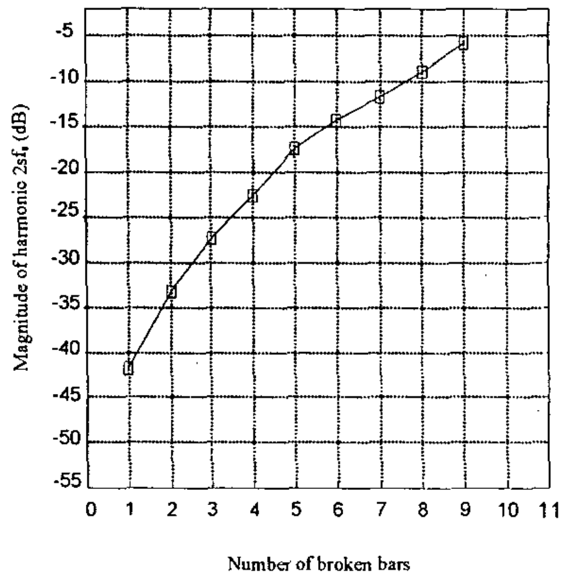

Fig.4 The magnitude of the $2sf_s$ component versus the number of adjacent broken bars.

Mr. A. Cruz [2], defined a normalized severity factor:

$$\text{normalized severity factor} = \frac{\text{Amplitude of the } 2gfs \text{ component}}{\text{dc level}}$$

Figure 5 shows that the normalized severity factor increases with the number of broken bars, making a good indicator of the operating conditions of the machine.

III. Experimental Tests

The test-motor used in the experimental investigation is a three phase, $50Hz$, 2-poles, $3Kw$, induction motor manufactured by Sew-Usocome drives a DC generator feeding a variable resistor provides a mechanical load (figure.6).

Figure 7 shows a rotor with one broken bar, used in the tests.

Figure 8 shows that in the absence of faults there exists some spectral components with small magnitude due to the inherent and natural asymmetries.

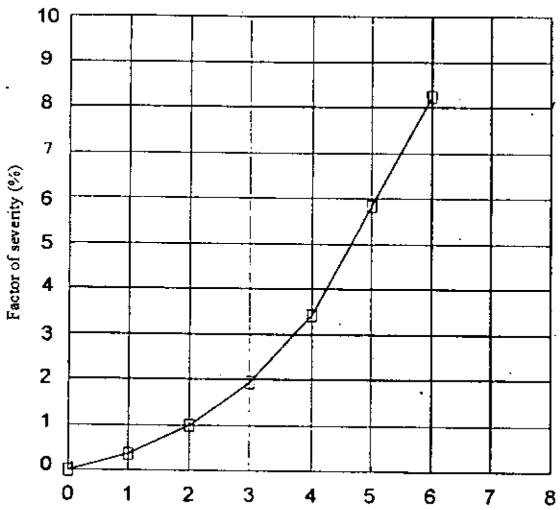

Fig.5 The behavior of the normalized severity factor according to the number of broken bars.

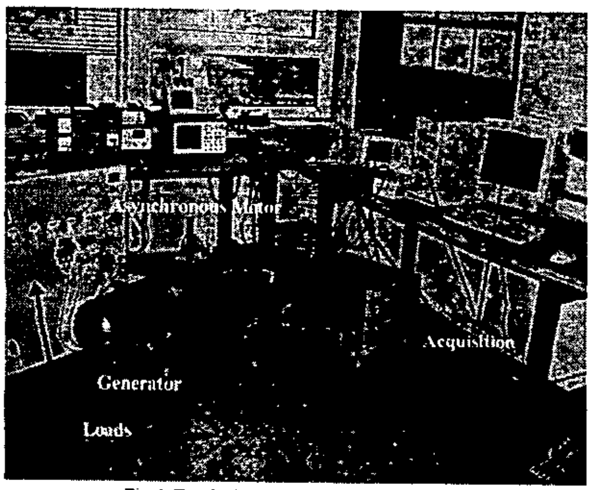

Fig.6 Test bed used for experimental results.

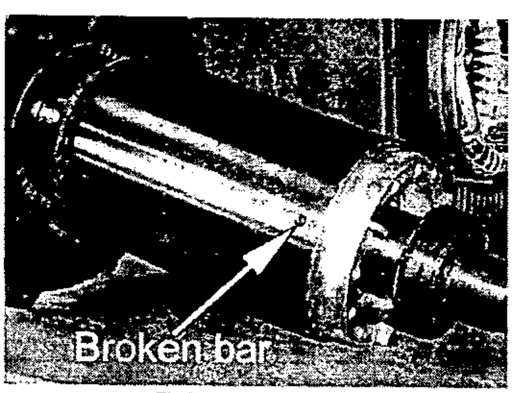

Fig.7 Rotor with broken bar.

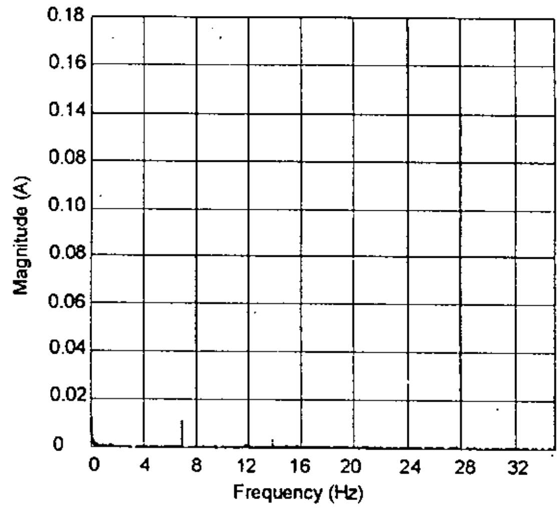

Fig.8 Experimental Spectrum of the ac level of current Park's vector modulus for a healthy motor with rated load (s=0.085)

As it was theoretically predicted, the occurrence of broken bar is characterized by the appearance of spectral components at the low frequencies of $2ksf_s$ (Figure 9).

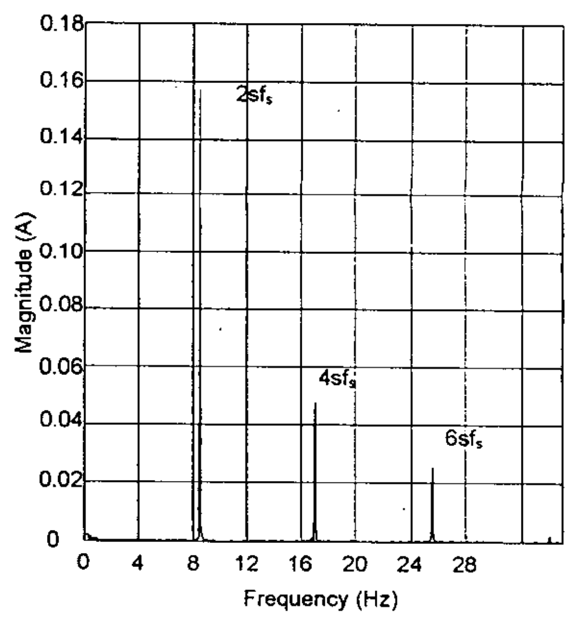

Fig.9 Experimental Spectrum of the ac level of current Park's vector modulus for a motor with one broken bar rated load (s=0.085)

IV. Conclusion

This paper shows that the occurrence of rotor cage faults can be effectively detected thanks to the Park's vector modulus analysis. With this approach, information is situated in low frequencies. Consequently, the Park's vector modulus provides easier filtering conditions. On the contrary, and when one uses the spectrum of the stator current for detecting rotor defects, it is sometimes difficult to distinguish the side bands $(1\pm 2s)f_s$ characterizing the bars defects, since these sidebands are at a distance from $\pm 2sf_s$ around the fundamental ($50Hz$) and this distance becomes very small with weak slip. Moreover this is also the same thing in case of high power induction motors.

It should be also notice that the taking into account of the currents in all three phases brings more information for the process of the diagnosis.

V. Acknowledgment

The authors wish to express their gratefulness to the Research Ministry and to Henri Poincaré University for their financial support in the development of the test-bed.

VI. Lists of symbols

i_m	the maximum value of the current
ω_s	the pulsation
i_f	the maximum value of the fundamental component of the current
i_l	the maximum value of the component lower $(1-2s)f_s$ of the current
i_r	the maximum value of the component higher $(1+2s)f_s$ of the current
α	the phase of the fundamental component of the current
β_l	the phase of the component $(1-2s)f_s$
β_r	the phase of the component $(1+2s)f_s$
s	the slip in per unit

VII. References

[1] A. J. M. Cardoso, S. M. A. Cruz, J. F. S. Carvallo and E. S. Saraiva, "Rotor Cage Fault Diagnosis in Three Phase Induction Motors by Park's Vector Approach", *Rec.IEEE Ind. Appl. Soc. Annu. Meet. Orlando, Florida*, vol. I, 1995, pp. 642-646.

[2] S. M. A. Cruz and A. J. M. Cardoso, , " Rotor Cage Fault Diagnosis in Three Phase Induction Motors by Extended Park's Vector Approach", *Electric Machines and Power Systems*, vol. 28, 2000, pp. 289-299.

[3] Alberto Bellini, F. Filippetti. and all, "Quantitative Evaluation of Induction Motor Broken Bars by Means of Electrical Signature Analysis," *IEEE Trans. On Industry Applications*, vol. 37, no 5, Sept/Oct. 2001, pp. 1248-1255.

[4] Andrzej M. Trzynadlowski and Ewen Ritchie, "Comparative Investigation of Diagnostic Media for Induction Motors : A Case of Rotor Cage Faults," *IEEE Transactions on Industry Electronics*, vol. 47, no. 5, October 2000, pp. 1092-1099.

[5] M. H. Benbouzid, M. Vieira and C. Theys "Induction Motors Faults Detection and Localization Using Stator Current Advanced Signal Processing Techniques", IEEE *Transactions on Industrial Electronics* vol 14, no1, Jan. 1999, pp. 14-22.

[6] R. R. Schoen, T.G. Habetler, F. Kamran and R. G. Bartheld, "Motor Bearing Damage Detection Using Stator Current Monitoring". *IEEE, Transactions on Industry Applications*, vol. 31, no. 6, Nov./Dec. 1995, pp. 1274-1279.

[7] S. E. Legowski, A. H. M. Sadrul Ula, Andrzej M. Trzynadlowski, "Instantaneous Power as Medium for the Signature Analysis of Induction Motors". *IEEE Transactions on Industry Applications*. vol. 32, no.4, July/August 1996, pp. 904-909.

[8] W. T. Thomson and M. Fenger, "Current Signature Analysis to Detect Induction Motor Faults". *IEEE Industry Application Magazine*, July/August 2001, pp. 26-34.

[9] J. S. Hsu, "Monitoring of Defects in Induction Motors Through Air-Gap Torque Observation", IEEE Transactions on Industry Applications, Vol. 31, No.5, Sept./Oct. 1995, pp. 1016-1021.

[10] J. R. Cameron and al. "Vibration and Current Monitoring for Detecting Air gap Eccentricity in Large Induction Motors". IEE Proceedings, Vol. 133, Pt. B, No. 3, May 1986. pp. 155-163.

[11] A. H. Bonnett and G. C. Soukup, "Cause and Analysis of Stator and Rotor Failures in Three-Phase Squirrel-Cage Induction Motors". *IEEE*

[12] *Transactions on Industry Applications*, vol. 28, no 4, July/August 1992, pp. 921-937.

[13] Y. Han and Y. H. Song, "Condition Monitoring Techniques for Electrical Equipment – A Literature Survey", *IEEE Transactions on Power Delivery*, vol. 18, no. 1, January 2003, pp. 4-13.

[14] G.B. Kliman and J. Stein. "Methods of Motor Current Signature Analysis", *Electric Machines and Power Systems*, vol. 20, no. 6, 1992, pp. 463-474.

[15] A. Jaco, A. Makki, H. Yahoui and G. Grellet, "Modeling of Three Phase Asynchronous Motor Application to Magnetic Faults Diagnostic", *ICEM 98*, Istanbul, Turkey, vol. 1, 1998, pp. 443-447